

# Hydroxylation of phenol over molybdovanadophosphoric acid modified zirconia

K.M. Parida\*, Sujata Mallick

*Colloids and Material Chemistry Department, Institute of Minerals and Materials Technology (CSIR),  
Bhubaneswar 751013, Orissa, India*

Received 20 August 2007; received in revised form 1 October 2007; accepted 3 October 2007  
Available online 9 October 2007

## Abstract

Molybdovanadophosphoric acid (MVPA) supported zirconia was synthesized by an incipient wetness impregnation method taking zirconium hydroxide and MVPA as the precursors. The neat and supported catalysts were calcined at 500 °C and characterized by nitrogen adsorption–desorption, X-ray powder diffraction, FTIR, UV–vis DRS, temperature programmed reduction (TPR) and Raman spectroscopy techniques. The 15 wt.% MVPA stabilizes the tetragonal phase of zirconia, which leads to an increase in surface area. The Keggin structure of MVPA remains unaltered up to 500 °C. The catalytic activities were evaluated for hydroxylation of phenol using H<sub>2</sub>O<sub>2</sub> as the oxidant. Among all the promoted catalysts, 15 wt.% molybdovanadophosphoric acid supported zirconia exhibits highest catalytic activity in phenol hydroxylation, giving 49% conversion having 61% *para* selectivity.

© 2007 Elsevier B.V. All rights reserved.

**Keywords:** Molybdovanadophosphoric acid; Phenol hydroxylation; Hydroquinone; Catechol

## 1. Introduction

Oxidation of phenol to hydroquinone (HQ) and catechol (CL) is an industrially interesting reaction, as the products have several important large-scale uses such as photographic film developer, antioxidant, polymerization inhibitor, medicines and organic synthesis, perfumes, etc. [1,2]. In addition, the quinone derivatives play an important role in bio-systems and find many miscellaneous industrial applications. Several soluble oxidizing agents either in stoichiometric quantity or catalytic amount have been used for the conversion of phenol into hydroquinone (*para*-dihydroxybenzene) and catechol (*ortho*-dihydroxybenzene) [3]. But the disadvantage found in most cases is the evolution of undesired toxic gases as well as liquid and solid wastes besides the process being highly expensive. Also in case of homogeneous catalytic process, hydroxylation of phenol gives very low *para* to *ortho* ratio. But the use of heterogeneous catalyst is a promising alternative to overcome this problem. The different solid acid tested so far include TiHMS [4,5], TiMCM-41 [4–6],

TiMMS [5], TS-1 [7], TiMMM [8], metal complexes [9] and polyoxometalates (POMs) [10–12]. Takehira and co-workers [11,12] reported the hydroxylation of phenols with 30% aqueous H<sub>2</sub>O<sub>2</sub> to produce hydroquinone and catechol using vanadium-containing POMs with Keggin structure.

The acid–base, redox behavior and well-known Keggin structure of POMs play an important role in synthesis and applications, especially homogeneous and heterogeneous catalysis. Their properties are dependent on the nature and the relative position of the metals in the framework because the acid and redox properties of POMs are controlled at the atomic and molecular levels by changing the constituent elements. Molybdenum and tungsten are the main constitutive metals in POMs. The general trends for the acid strengths of these Keggin acids are W > Mo (for polyatom) and P<sup>5+</sup> > Si<sup>4+</sup> (for the heteroatom) [13]. The oxidation potential (or oxidizing ability) has been reported to be in the order: [PMo<sub>12</sub>O<sub>40</sub>]<sup>3–</sup> > [SiMo<sub>12</sub>O<sub>40</sub>]<sup>4–</sup> > [PW<sub>12</sub>O<sub>40</sub>]<sup>3–</sup> > [SiW<sub>12</sub>O<sub>40</sub>]<sup>4–</sup> [14]. In addition, the introduction of vanadium (V) into the Keggin framework [PMo<sub>12</sub>O<sub>40</sub>]<sup>3–</sup> is beneficial for redox catalysis [15], shifting its reactivity from acid dominated to redox dominated, as demonstrated by the selective oxidation of methanol to either dimethyl ether or formaldehyde [16] and

\* Corresponding author.

E-mail address: [kmparida@yahoo.com](mailto:kmparida@yahoo.com) (K.M. Parida).

by other selective oxidation of alkanes and aldehydes [17–20]. However, the disadvantage of POMs as catalysts is their low surface area and low thermal stability. To minimize these disadvantages, the POMs were supported on different carriers and also, impregnating solutions in different solvents were employed [21].

It should be noted that in the literature, practically there are many papers on heteropoly acid as catalyst for hydroxylation of phenol but no data is available on molybdovanadophosphoric acid supported on zirconia. Our paper is the first attempt to evaluate the catalytic activity of molybdovanadophosphoric acid supported on zirconia for hydroxylation of phenol.

## 2. Experimental

### 2.1. Preparation of zirconia

Zirconium hydroxide gel was prepared from zirconium oxychloride aqueous solution (S. D. Fine Chemicals Ltd.) by drop wise addition of ammonium hydroxide solution (25% ammonia) (Merck Specialities Private Limited) up to pH 9.5. The hydrogel was refluxed for 24 h, then filtered and washed with deionized water and dried in an oven at 120 °C for 24 h and crushed to fine powders. Then it was calcined at 500 °C for 5 h (named Z herein after) and kept in desiccator for further use.

### 2.2. Preparation of phosphomolybdic acid and molybdovanadophosphoric acid

#### 2.2.1. Preparation of phosphomolybdic acid

Ammonium heptamolybdate (20 g) (Merck Specialities Private Limited) was dissolved in dilute H<sub>3</sub>PO<sub>4</sub>. Then it was acidified with concentrated HCl till complete formation of yellow precipitation. It was then filtered and washed with distilled water and dried in an oven at 70 °C.

#### 2.2.2. Preparation of molybdovanadophosphoric acid

First 22.3 g of MoO<sub>3</sub> (Aldrich, 99.5% pure) and 1.3 g V<sub>2</sub>O<sub>5</sub> (Aldrich 99.6% pure) were added to 350 ml of distilled water. The mixture was refluxed for 1 h. Then 1.7 g of 85% phosphoric acid (Aldrich) was added in three equal aliquots, approximately 10 min apart. After addition of phosphoric acid, another 150 ml of distilled water was added to the flask. The mixture was allowed to reflux for 16 h with vigorous stirring and a bright orange solution was formed. The liquid in the flask was evaporated and a bright orange solid was obtained.

X-ray fluorescence analysis showed that Mo to V ratio in molybdovanadophosphoric acid sample is 11:1.

### 2.3. Preparation of molybdovanadophosphoric acid and phosphomolybdic acid supported zirconia

A series of catalysts having different loading from 3 to 20 wt.% were synthesized by impregnating 2 g of Z with an aqueous solution of molybdovanadophosphoric acid (MVPA) (0.06–0.30 g/10–50 ml of conductivity water) under constant

stirring followed by heating at 100 °C till complete evaporation (4 h). Then it was dried in oven at 110 °C for 24 h. Catalysts with different MVPA loading from 3 to 20 wt.% were then calcined at 500 °C. The catalysts will be herein after referred to *x*ZMVPA (*x* = 3–20 wt.%). Similarly, 15 wt.% PMA supported zirconia was also prepared for comparison purpose with 15 wt.% ZMVPA.

### 2.4. Physico-chemical characterization

The BET surface area and pore size distribution were determined by multipoint N<sub>2</sub> adsorption–desorption method at liquid N<sub>2</sub> temperature (–196 °C) by a Sorptomatic 1990 (Thermo-Quest, Italy). Prior to analyses, all the samples were subjected to vacuum at 200 °C to ensure a clean surface.

The X-ray powdered diffraction pattern was recorded on a Philips PW 1710 diffractometer with automatic control. The patterns were run with a monochromatic Cu K $\alpha$  radiation with a scan rate of 2° min<sup>–1</sup>.

The FTIR spectra were taken using Jasco FTIR 5300 in KBr matrix in the range of 400–4000 cm<sup>–1</sup>.

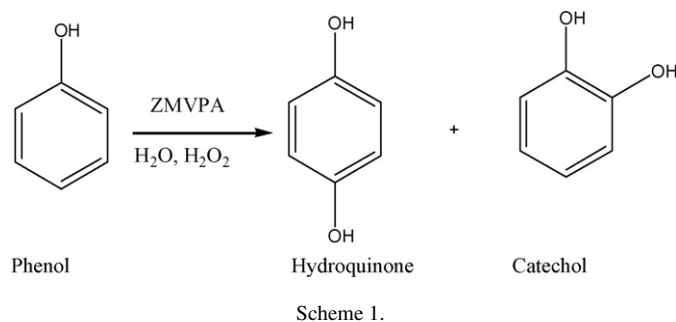
The UV–vis spectra of the samples were recorded in a Varian UV–vis DRS spectrophotometer fitted with Carry 1E software. The spectra were recorded against the boric acid as reference.

The H<sub>2</sub>-TPR of all the samples was carried out in a CHEMBET-3000 (Quantachrome, USA) instrument. About 0.1 g sample was taken inside quartz ‘U’ tube and degassed at 350 °C for 1 h with helium gas flow. The sample was then cooled to 30 °C and at this temperature the gas flow was changed to 5% H<sub>2</sub> in nitrogen. It was then heated at a heating rate of 10 °C/min up to 800 °C and the spectra were recorded.

Raman spectra were obtained on inVia Raman microscope (Renishaw, UK) equipped with a counter current detector (CCD). The spectra were recorded using 514.5 nm excitation lines from an argon ion laser with a spectral resolution of 1 cm<sup>–1</sup>.

### 2.5. Catalytic activity

The oxidation of phenol was carried out in a round bottom flask equipped with a reflux condenser. About 5 mmol of the substrate was dissolved in 15 ml of deionized water and 0.05 g of the catalyst was added to it. To this mixture, 5 mmol of aqueous H<sub>2</sub>O<sub>2</sub> (30%) was added drop wise. The reaction mixture was stirred for 2 h at 60 °C (Scheme 1). The reaction products were analyzed off-line by gas chromatography (Shimadzu GC-17A)



through capillary column (ZB-1, 30 m length, 0.53 mm I.D. and 3.0  $\mu\text{m}$  film thickness) using Flame ionization Detector (FID).

### 3. Results and discussion

#### 3.1. Characterization

Table 1 shows the BET surface area of neat and different weight percentage of ZMVPA samples. Zirconium oxyhydroxide dried at 120 °C showed a surface area 412  $\text{m}^2/\text{g}$ . After calcinations at 500 °C, the surface area drastically decreased to 142  $\text{m}^2/\text{g}$ . Addition of MVPA on zirconia results in an increase of the surface area. The 15 wt.% MVPA loaded zirconia show maximum surface area 229  $\text{m}^2/\text{g}$ . However, on further loading, the surface area decreases. This implies that the presence of MVPA plays a prominent role in making the material porous. The added MVPA strongly interact with zirconia reducing surface diffusion of zirconia and so inhibits sintering. It stabilized the tetragonal phase of zirconia, which leads to an increase in surface area. However, when the MVPA content increases beyond 15 wt.%, pore blocking takes place due to the presence of an excess amount of molybdovanadophosphoric acid.

The nitrogen adsorption–desorption isotherms of parent zirconia and 15 wt.% ZMVPA were shown in Fig. 1a and b, respectively. The isotherms are very much similar to the type IV isotherm according to the IUPAC classification of adsorption isotherms [22], which is a typical characteristic of mesoporous solids. Inflections at  $P/P_0$  0.4–0.6 for 15 wt.% ZMVPA and at 0.45–0.65 for parent zirconia were seen in the figure, which are due to the spontaneous filling of mesopores due to capillary condensation.

Fig. 2 shows the BJH pore size distribution of zirconia and 15 wt.% ZMVPA. From the figure one can see that there is no appreciable change in pore diameter by incorporation of 15 wt.% ZMVPA on zirconia.

The XRD patterns of zirconia and ZMVPA samples are presented in Fig. 3. It was observed that pure zirconia contains mixture of tetragonal and monoclinic phases with the latter as the major constituents. However, XRD of low MVPA loading samples is similar to that of the support. As percentage loading

Table 1

Surface area, conversion and selectivity of various catalysts towards hydroxylation of phenol

Catalysts	Surface area ( $\text{m}^2/\text{g}$ )	Conversion (%)	Selectivity (%)	
			HQ	CL
Z	142	5	45.3	54.6
3 wt.% ZMVPA	154	12	49.5	50.3
6 wt.% ZMVPA	165	22	50.2	49.6
9 wt.% ZMVPA	190	35	52.9	46.5
12 wt.% ZMVPA	199	41	56.3	43.1
15 wt.% ZMVPA	229	49	60.6	39.3
20 wt.% ZMVPA	213	46	62.8	37.1
15 wt.% ZPMA	211	5	24	75

Phenol (5 mmol),  $\text{H}_2\text{O}_2$  (5 mmol), catalyst (0.05 g) and water (15 ml), time 2 h, HQ: hydroquinone and CL: catechol.

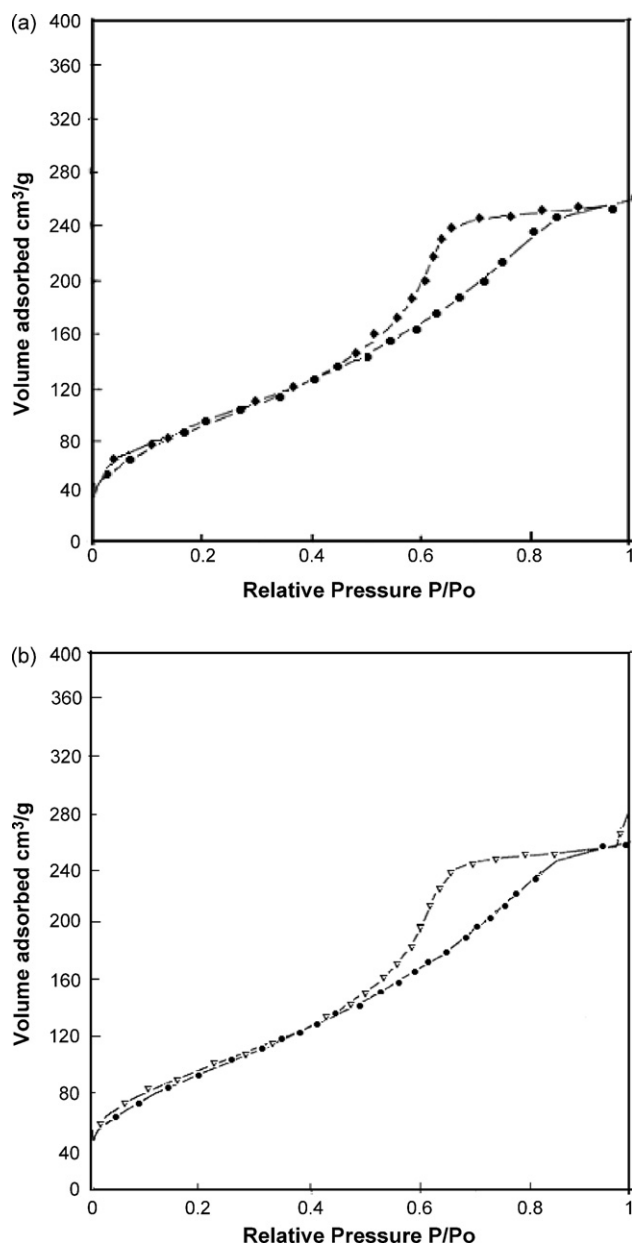


Fig. 1. (a)  $\text{N}_2$  adsorption ( $\blacklozenge$ ) and desorption ( $\bullet$ ) isotherms of zirconia. (b)  $\text{N}_2$  adsorption ( $\triangle$ ) and desorption ( $\bullet$ ) isotherms of 15 wt.% ZMVPA.

of MVPA increases, it shows increase in tetragonal phase while 15 wt.% ZMVPA is fully tetragonal. But on further increase in MVPA loading, it shows monoclinic along with tetragonal.

Fig. 4 shows the UV–vis DRS spectra of (a) zirconia, (b) 15 wt.% ZPMA and (c) 15 wt.% ZMVPA samples calcined at 500 °C. The zirconia (Fig. 4a) exhibits a strong absorption band at 230 nm, which may be attributed to the charge transfer from oxide species to zirconium cation ( $\text{O}^- \rightarrow \text{Zr}^{4+}$ ). In contrast, the spectra of both 15 wt.% ZPMA and 15 wt.% ZMVPA show broad band at 250 nm which match well with the literature values [23], suggesting thereby the presence of undegraded  $\text{H}_3\text{PM}_{12}\text{O}_{40}$  species. An additional band is found at 308 nm in compared with ZPMA, indicating the incorporation of vanadium into the Keggin ion [24].

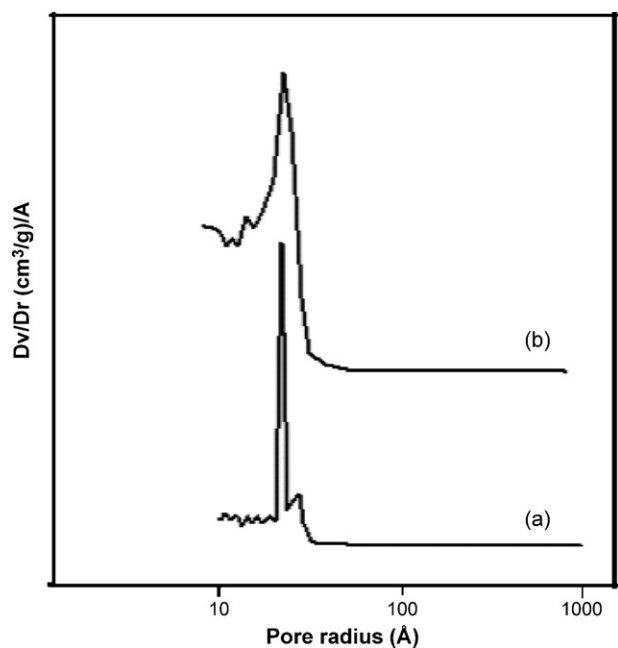


Fig. 2. Distribution of pore size as a function of pore radius of (a) zirconia and (b) 15 wt.% of ZMVPA.

The FTIR spectra of zirconia, 15 wt.% ZPMA and 15 wt.% ZMVPA calcined at 500 °C are presented in Fig. 5. The FTIR spectrum of Z shows broad band in the region of 3410  $\text{cm}^{-1}$  due to asymmetric stretching of OH group and two bands at

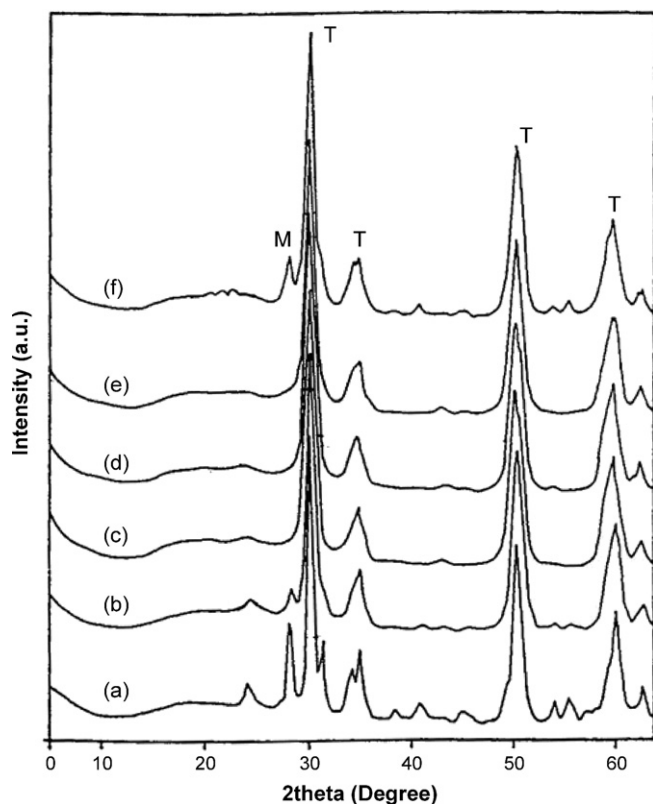


Fig. 3. XRD patterns of (a) Z, (b) 6 wt.% ZMVPA, (c) 9 wt.% ZMVPA, (d) 12 wt.% ZMVPA, (e) 15 wt.% ZMVPA and (f) 20 wt.% ZMVPA (calcined at 500 °C).

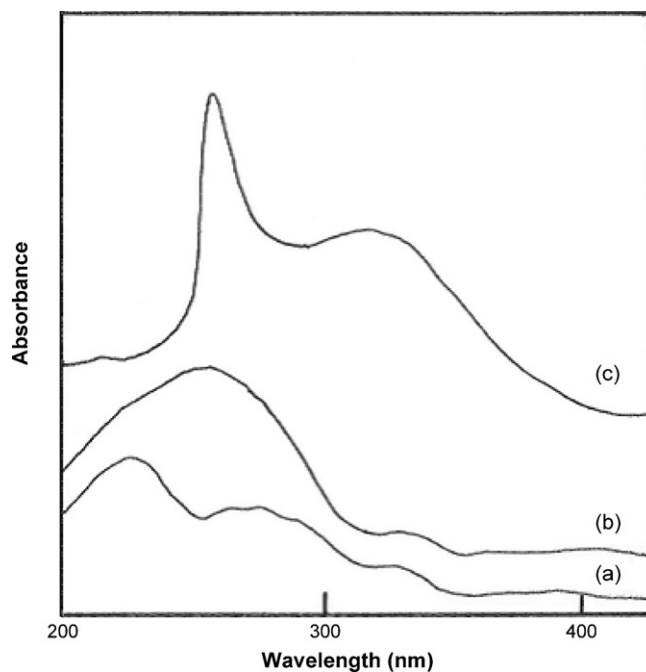


Fig. 4. UV-vis spectra of (a) Z, (b) 15 wt.% ZPMA, and (c) 15 wt.% ZMVPA.

1621 and 1386  $\text{cm}^{-1}$  which are due to bending vibration of  $-(\text{H}-\text{O}-\text{H})-$  and  $-(\text{O}-\text{H}-\text{O})-$  bond. The band at 600  $\text{cm}^{-1}$  is attributed to the presence of  $\text{Zr}-\text{O}-\text{H}$  bond (Fig. 5a). In addition to these bands, the FTIR spectra of 15 wt.% ZPMA (Fig. 5b) show bands 1059, 888, 789  $\text{cm}^{-1}$  assigned to the symmetric stretching of  $\text{P}-\text{O}$ ,  $\text{Mo}-\text{O}_c-\text{Mo}$ ,  $\text{Mo}-\text{O}_e-\text{Mo}$  respectively and a weak shoulder at 954  $\text{cm}^{-1}$  due to  $\text{Mo}-\text{O}_t$ , confirmed the presence of the undegraded phosphomolybdic acid. Here, 't' tends for the terminal oxygen bonding to one Mo atom, 'c' for the corner sharing oxygen atom connecting  $\text{Mo}_3\text{O}_{13}$  units and 'e' for the edge sharing oxygen-connecting Mo [25]. There is slight shifting of bands in FTIR spectra of 15 wt.% ZMVPA sample (Fig. 5c) which indicates that the Keggin phase remains unaltered after the incorporation of vanadium into the Keggin ion [26].

Fig. 6 gives the  $\text{H}_2$ -TPR profiles obtained from the various catalysts. It was observed that no  $\text{H}_2$  consumption was recorded for the zirconia support. The support reducibility seems to have

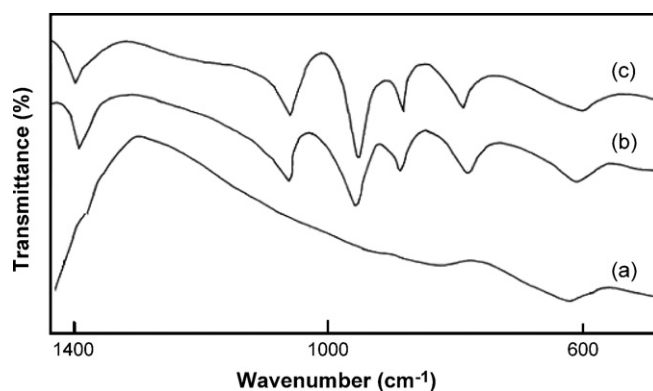


Fig. 5. FTIR spectra of (a) Z, (b) 15 wt.% ZPMA, and (c) 15 wt.% ZMVPA.

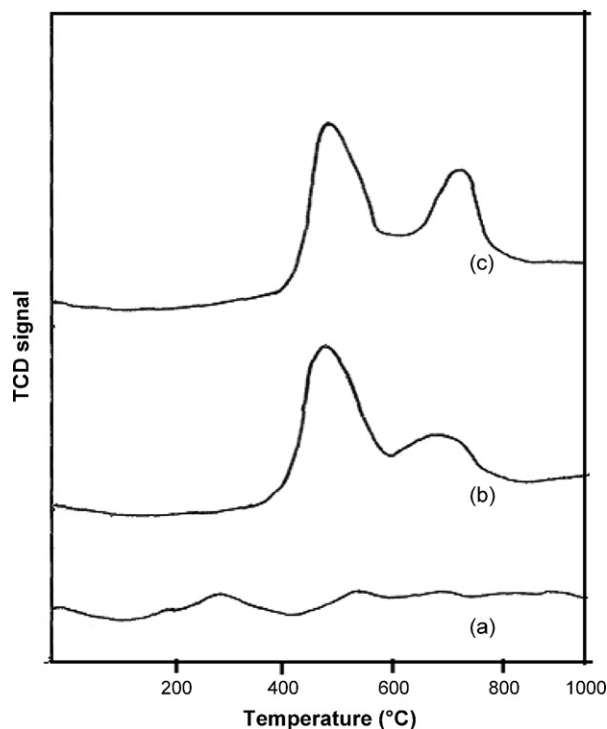


Fig. 6. TPR spectra of (a) zirconia, (b) 15 wt.% ZPMA and (c) 15 wt.% ZMVPA.

been modified in the presence of PMA and MVPA on zirconia. TPR pattern of ZPMA and ZMVPA catalysts are similar, since they consist of two main reduction peaks observed at temperature around 450 and 695 °C. Introduction of a vanadium atom in anion or in countercation position of heteropoly molybdates makes reduction of molybdenum species easier. The reduction up to 450 °C could also include reduction of vanadium containing species. The second main peak (at about 695 °C) is probably connected with a deeper reduction of Mo species ( $\text{HPMo}_{12}$ ) and/or with reduction of a new phase containing V and P.

Raman spectra of zirconia and 15 wt.% ZMVPA promoted zirconia samples are shown in Fig. 7. Normally, crystalline zirconia exhibits characteristic Raman bands in the 500–700  $\text{cm}^{-1}$  region. From Fig. 7, the spectra of zirconia reveal the Raman bands pertaining to a mixture of monoclinic (221, 331, 380, 478 and 639  $\text{cm}^{-1}$ ) and tetragonal (290, 312, 455, 645  $\text{cm}^{-1}$ ) phases.

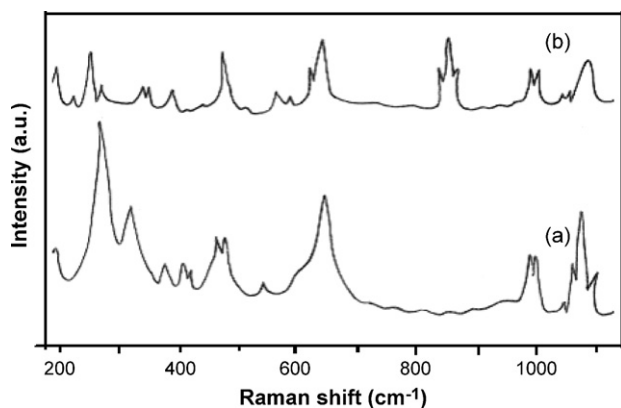


Fig. 7. Raman spectra of the catalyst (a) zirconia and (b) 15 wt.% ZMVPA.

The spectra of MVPA supported zirconia sample reveals relatively intense Raman bands pertaining to the tetragonal phase. Further, a broad band observed at 1059  $\text{cm}^{-1}$  could be attributed to the anti-symmetric  $\text{PO}_4$  stretching mode. In addition, the Raman bands due to the Mo–Oxygen stretching vibration can be seen at 987, 970 and 830  $\text{cm}^{-1}$ . The band at 250  $\text{cm}^{-1}$  is assigned to the Mo–O–Mo bending modes of the intact Keggin structure.

### 3.2. Hydroxylation of phenol

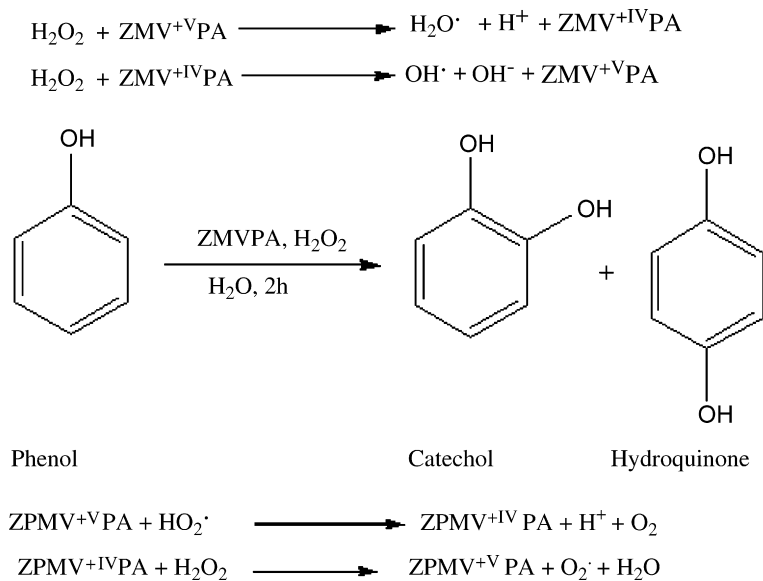
The conversion of phenol and selectivity to hydroquinone and catechol over modified zirconia systems at 60 °C in presence of hydrogen peroxide in water medium is shown in Table 1. Vanadium free phosphomolybdic acid supported on zirconia (15 wt.% ZPMA) showed very low activity (5%) compared to vanadium-containing phosphomolybdic acid (15 wt.% ZMVPA), however, the former show remarkably high *ortho* selectivity. This indicates that vanadium atom located in the Keggin structure enhanced the oxidative activity. It is observed that among different loading of molybdovanadophosphoric acid on zirconia, the 3 wt.% ZMVPA showed 12% conversion having 49% *para*, 50% *ortho* selectivity. The conversion increased to a maximum of 49% conversion having 61% *para*, 39% *ortho* selectivity at 15 wt.% loading. On further increasing the weight percentage to 20 wt.%, the conversion decreases to 46%. For 15 wt.% loading there is monolayer coverage of MVPA on the support. But above 15 wt.% there is over loading of MVPA and some pores of zirconia are blocked.

The reaction mechanism for the oxidation of aromatic compounds employing transition metals has been studied by others [21,27]. The reaction path for the present study involves the interaction of ZMVPA catalysts with  $\text{H}_2\text{O}_2$  yields  $\text{OH}^\bullet$  and  $\text{HO}_2^\bullet$  species via a redox mechanism. Then the  $\text{OH}^\bullet$  radical attacks the phenol ring and yields hydroquinone and catechol as the major product. Oxygen and water are formed as the side products by the decomposition of the hydrogenperoxi radical and  $\text{H}_2\text{O}_2$ , respectively. So the reaction mainly follows free radical mechanism (Scheme 2).

Generally, the catalytic activity and product selectivity in phenol hydroxylation by hydrogen peroxide are strongly influenced by surface area of the catalyst, solvents, reaction time, reaction temperature, molar ratio of phenol to hydrogen peroxide, and catalyst amount, which are investigated systematically as follows on 15 wt.% ZMVPA.

#### 3.2.1. Influence of the solvents

The solvents used in the catalytic reaction are known to have a profound influence on phenol conversion and the ratio of hydroquinone to catechol over titanium silicates [28,29] and vanadium silicates-2 [30]. The influence of solvents on conversion and selectivity of the reaction over 15 wt.% ZMVPA is illustrated in Table 2. When 1,2-dichloroethane is used as a solvent, the catalytic reaction does not take place. In case of acetone or in ethanol low conversion is observed, while in case of acetonitrile the conversion was found to be 22%. In water, both phenol and  $\text{H}_2\text{O}_2$  dissolved easily and active hydroxyl radicals can be



Scheme 2.

Table 2  
Influence of solvent on hydroxylation of phenol reaction

Solvent	Conversion (%)	Selectivity (%)	
		Hydroquinone	Catechol
1,2-Dichloroethane	2	20.3	78.9
Acetonitrile	22	48.2	50.6
Acetone	8	60.4	39.3
Ethanol	6	49.2	50.0
Water	49	60.6	39.4

Phenol (5 mmol), H<sub>2</sub>O<sub>2</sub> (5 mmol), catalyst (0.05 g) and water (15 ml), time 2 h.

formed. This effect of the solvents strongly supports that radical reaction mechanism is in operation in phenol hydroxylation. Radicals generated are more stable in polar solvents. As ethanol is a well-known scavenger of hydroxyl radical, negligible reaction conversion took place.

### 3.2.2. Influence of reaction time

The dependence of catalytic activity on reaction time was shown in Fig. 8. It was found that the percentage of conver-

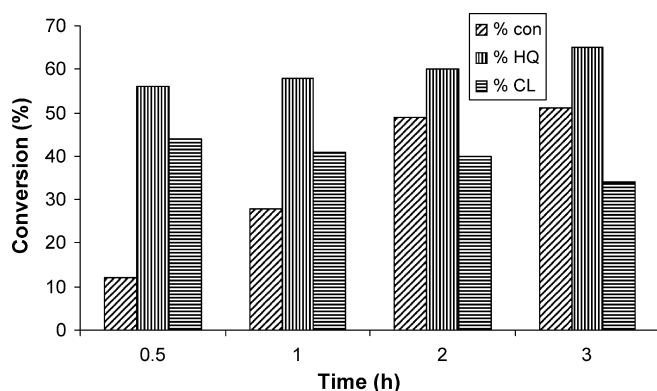


Fig. 8. Effect of time on conversion of phenol using 15 wt.% ZMVPA as catalyst (0.05 g) phenol (5 mmol), H<sub>2</sub>O<sub>2</sub> (5 mmol), and acetic acid (5 ml).

sion increases from 12 to 49% with increase in reaction time from 0.5 to 2 h and then remains almost constant with further rise of reaction time up to 3 h. This indicated that the optimized reaction conditions are more favorable than the reported ones as much longer reaction time was employed while less hydroquinone and catechol yield were obtained. In case of selectivity ratio (HQ/CL), it increases from 1.27 to 1.98.

### 3.2.3. Influence of reaction temperature

The influence of reaction temperature on the hydroxylation of phenol is shown in Fig. 9. The reaction was carried out in the temperature region 40–90 °C over 15 wt.% ZMVPA as catalyst while keeping the other parameters fixed. The percentage of conversion of phenol increased from 38 to 51 with the increase in temperature from 40 to 80 °C. This is due to the fact that H<sub>2</sub>O<sub>2</sub> decomposition increases with the increase in temperature. This indicates that higher temperature up to 80 °C is beneficial for the hydroxylation of phenol. But above 80 °C, the conversion of phenol is decreased due to enhanced H<sub>2</sub>O<sub>2</sub> decomposition. The same trend was also reported by Jang and

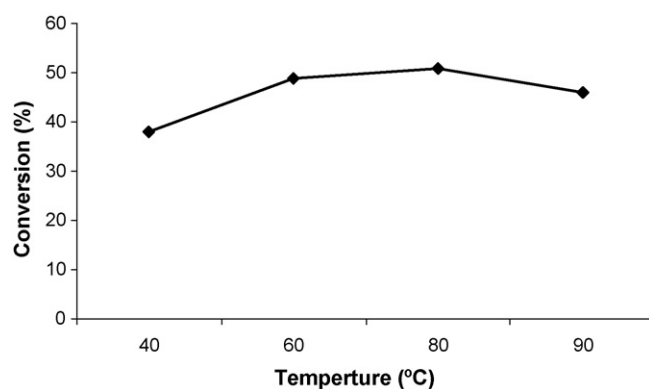


Fig. 9. Effect of temperature on conversion of phenol using 15 wt.% ZMVPA as catalyst (0.05 g), phenol (5 mmol), H<sub>2</sub>O<sub>2</sub> (5 mmol), and acetic acid (5 ml).

Table 3  
Hydroxylation of phenol over 15 wt.% ZMVPA and comparison of the result with other reported methods

Catalyst used	Time (min)	Conversion (%)	Selectivity (%)		Reference
			HQ	CL	
ZMVPA	120	49	60	39	[This method]
Fe-MCM-41	10	60	32	68	[31]
TS-1	720	27	50	50	[33]
Modified zeolite	360	43	12	88	[34]

co-workers [31] over Fe-MCM-41 as catalyst. Table 3 represents comparative feature between the performance of ZMVPA and other reported catalysts for hydroxylation of phenol. Catalytic activity of our catalyst is comparable to other reported catalysts in terms of conversion and hydroquinone, catechol selectivity.

### 3.2.4. Influence of molar ratio of phenol/H<sub>2</sub>O<sub>2</sub>

The activity of hydroxylation of phenol in different phenol/H<sub>2</sub>O<sub>2</sub> molar ratio is shown in Fig. 10. It is observed from the figure that the conversion of phenol is higher at lower phenol/H<sub>2</sub>O<sub>2</sub> ratio. On the other hand increase in selectivity of catechol and decrease in phenol conversion is observed with the increase in phenol/H<sub>2</sub>O<sub>2</sub> molar ratio. Similar results also reported by Neuman et al. [32]. The coordination of H<sub>2</sub>O<sub>2</sub> on the metal, and its subsequent decomposition to OH• radical were the necessary steps in this reaction as described above. At the molar ratio of 1, H<sub>2</sub>O<sub>2</sub> could freely coordinate to metal and decompose to form OH• radical. Hence, high phenol conversion was attained. At the molar ratio of 2, low amount of H<sub>2</sub>O<sub>2</sub> must compete with excess phenol for coordination, and hence formation of OH• radicals might be significantly reduced. Thus, the conversion decreased.

### 3.2.5. Influence of catalyst amount

The variation of the catalytic activity with the amount of catalyst is shown in Fig. 11. It is observed that with increasing the amount of catalyst from 0.025 to 0.05 g the phenol conversion enhanced from 32 to 49%. Further increment of catalyst amount to 0.1 g resulted in only a marginal increase in phenol conversion (51%).

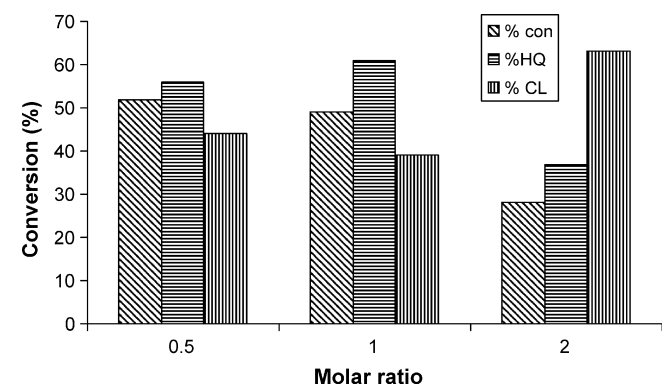


Fig. 10. Effect of molar ratio of phenol/H<sub>2</sub>O<sub>2</sub> on conversion of phenol using 15 wt.% ZMVPA as catalyst (0.05 g), and acetic acid (5 ml).

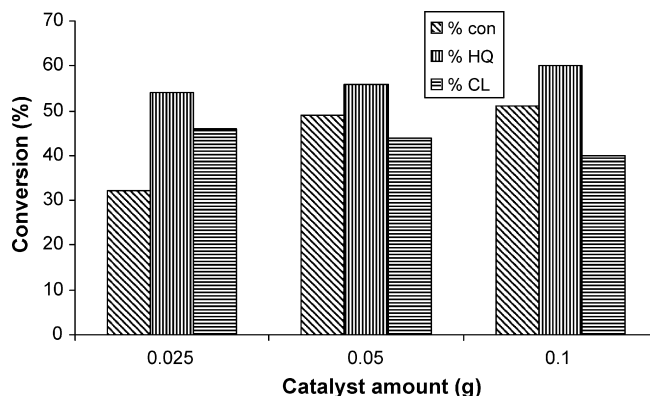


Fig. 11. Effect of catalyst amount on conversion of phenol using 15 wt.% ZMVPA as catalyst (0.05 g phenol (5 mmol), H<sub>2</sub>O<sub>2</sub> (5 mmol), and acetic acid (5 ml)).

### 3.3. Recyclability of the catalyst

The catalyst with 15 wt.% loading was used for recycling experiments. In order to regenerate the catalyst after 2 h of reaction, it was separated by filtration, washed with conductivity water several times, dried at 110 °C and calcined at 500 °C and used in the hydroxylation of phenol with a fresh reaction mixture. In the regenerated sample after two cycles, the yield decreases by 4%.

## 4. Conclusions

XRD and Raman spectra results indicated that the presence of MVPA retarded the crystallization of zirconia and stabilized ZrO<sub>2</sub> in tetragonal phase. Nitrogen adsorption–desorption studies revealed that the modified MVPA samples retain the mesoporosity, where as there is no appreciable change in pore diameter after impregnation of MVPA on zirconia. It is confirmed from FTIR and Raman spectra that the molybdovanadophosphoric acid keeps its Keggin type structure when supported on zirconia. TPR spectra revealed that the introduction of a vanadium atom in anion or in counteranion position of heteropoly molybdates makes reduction of molybdenum species easier. Vanadium atom located in the Keggin structure enhanced the catalysts oxidative activity towards hydroxylation of phenol. Among all the promoted catalyst, 15 wt.% of molybdovanadophosphoric acid impregnated on zirconia showed higher catalytic activity and having 61% *para* selectivity. Molybdovanadophosphoric acid supported on zirconia acts as an efficient and stable solid acid catalyst for hydroxylation of phenol.

## Acknowledgements

The authors are thankful to Prof. B.K. Mishra Director, Regional Research Laboratory (CSIR), Bhubaneswar for his constant encouragement and permission to publish this paper. Mrs. Sujata Mallick is obliged to CSIR for the award of SRF. DST is gratefully acknowledged for the financial support.

## References

- [1] P. Schudel, H. Mayer, O. Isler, W.H. Sebrell, R.S. Harris (Eds.), *The Vitamins*, vol. 5, Academic Press, New York, 1972, pp. 165–317.
- [2] K. Weissmehl, H.J. Arpe, *Industrial Organic Chemistry*, VCH, Weinheim, 1993, pp. 358.
- [3] R.A. Sheldon, R.A. Van Santen (Eds.), *Catalytic Oxidation: Principles and Applications*, World Scientific, Singapore, 1995, pp. 79–93.
- [4] P.T. Tanev, M. Chibwe, T.J. Pinnavaia, *Nature* 368 (1994) 321–323.
- [5] W.S. Ahn, N.K. Kim, S.Y. Jeong, *Catal. Today* 68 (2001) 83–88.
- [6] A. Corma, M.T. Navro, J. Perez-Pariente, *J. Chem. Soc., Chem. Commun.* (1994) 147–148.
- [7] B. Notari, *Stud. Surf. Sci. Catal.* 37 (1988) 413–425.
- [8] N.N. Trukhan, V.N. Romannikov, E.A. Paukshtis, A.N. Shmakov, O.A. Kholdeeva, *J. Catal.* 202 (2001) 110–117.
- [9] Q.S. Liu, J.F. Yu, Z.L. Wang, P.P. Yang, T.H. Wu, *React. Kinet. Catal. Lett.* 73 (2001) 179–186.
- [10] M. Shimizu, H. Orita, T. Hayakawa, Y. Watanabe, K. Takehira, *Bull. Chem. Soc. Jpn.* 63 (1990) 1835–1837.
- [11] M. Shimizu, H. Orita, T. Hayakawa, Y. Watanabe, K. Takehira, *Bull. Chem. Soc. Jpn.* 64 (1991) 2585–2587.
- [12] M. Shimizu, H. Orita, T. Hayakawa, K. Takehira, *Tetrahedron Lett.* 30 (1989) 471–474.
- [13] M. Misono, *Catal. Rev. Sci. Eng.* 29 (1987) 269–321.
- [14] I.V. Kozhevnikov, *Catal. Rev.* 98 (1998) 171–198.
- [15] N. Mizuno, M. Misono, *J. Mol. Catal.* 86 (1994) 319–342.
- [16] J. Melsheimer, S.S. Mahmoud, G. Mestl, R. Schlogl, *Catal. Lett.* 60 (1999) 103–111.
- [17] I.V. Kozhevnikov, *Catal. Rev.-Sci. Eng.* 37 (1995) 311–352.
- [18] O. Watzenberger, G. Emig, D.T. Lyuch, *J. Catal.* 124 (1990) 247–258.
- [19] Y. Seki, J.S. Min, M. Misono, N. Mizuno, *J. Phys. Chem. B* 104 (2000) 5940–5944.
- [20] K. Nomiya, K. Hashino, Y. Nemoto, M. Watanabe, *J. Mol. Catal. A* 176 (2001) 79–86.
- [21] M. Fournier, R. Thouvenot, C. Rocchiccioli-Deltch, *J. Chem. Soc. Faraday Trans.* 87 (1991) 349–356.
- [22] K.S.W. Sing, D.H. Everett, R.A.W. Haul, L. Moscou, R.A. Pierotti, J. Rouquerol, T. Siemieniewska, *Pure Appl. Chem.* 57 (1985) 603–619.
- [23] T. Okuhura, N. Mizuno, M. Misono, *Adv. Catal.* 41 (1996) 113–252.
- [24] G.A. Tsigdinos, C.J. Hallada, *Inorg. Chem.* 7 (1968) 437–441.
- [25] F. Babou, G. Coudurier, J.C. Vedrine, *J. Catal.* 152 (1995) 341–349.
- [26] B.B. Bardin, R.J. Davis, *Appl. Catal. A* 185 (1999) 283–289.
- [27] G. Goor, J. Edwards, R. Curu, in: G. Strukul (Ed.), *Catalytic Oxidations with Hydrogen Peroxide as Oxidant*, 50, Kluwer Academic Publishers, Dordrecht, 1993, pp. 423–425.
- [28] U. Romano, A. Esposito, F. Maspero, C. Neri, M.G. Clerci, *Chem. Ind. (Milan)* 72 (1990) 610–616.
- [29] A. Teol, S. Moussa-Khou Zami, Y. Ben Tarit, C. Naccache, *J. Mol. Catal.* 68 (1991) 45–52.
- [30] P.R. Hari, P. Rao, A.V. Ramaswamy, *Appl. Catal. A* 93 (1993) 123–130.
- [31] J.S. Choi, S.S. Yoon, S.H. Jang, W.S. Ahn, *Catal. Today* 111 (2006) 280–287.
- [32] R. Neumann, M. Levin-Elad, *Appl. Catal. A* 122 (1995) 85–97.
- [33] S.K. Mohapatra, F. Hussain, P. Selvem, *Catal. Commun.* 4 (2003) 57–62.
- [34] M.R. Maurya, S.J.J. Titinchi, S. Chand, *J. Mol. Catal.* 214 (2004) 257–264.